COMPARATIVE THERMAL AND FLOW ANALYSES OF TWO DIFFERENT PLATE PATTERNS FOR A COMPACT PLATE HEAT EXCHANGER

Barış Gürel [1], Ali Keçebaş [2,*], Volkan Ramazan Akkaya [2], Merve Göltaş [2], Karani Kurtuluş [1], Onur Vahip Güler [2]

[1]Süleyman Demirel University, Department of Mechanical Engineering, Isparta, Turkey

[2]Muğla Sıtkı Koçman University, Department of Energy Systems Engineering, Muğla, Turkey

*Corresponding Author: alikecebas@mu.edu.tr

ABSTRACT

It is known that the most significant difference of plate heat exchangers (PHEs) from other heat exchangers (HEs) is their heat transfer efficiency. The thinness of the plates separating the two fluids compared to the other HEs increases the heat transfer rate and decreases the heat losses that will occur during the transfer. Since heat rejection is an essential part of Organic Rankine Cycle (ORC) systems, all improvements on heat transfer will lead higher efficiencies. The aim of the study is to increase the efficiency of PHEs. In this study, two different compact PHE prototypes with trachea pattern and fish gill pattern are created by taking inspiration from nature. HEs are made up of three plates each. PHEs are numerically analyzed using computational fluid dynamics (CFD). Temperature and pressure contours are taken for both the hot and cold sides, and the convective heat transfer coefficient, Reynold's number, Prandtl number, effectiveness and entropy generation are calculated. The results obtained are compared. The heat transfer amount for the trachea patterned PHE was 2800W, entropy production 27.07W/K, effectiveness 0.26, while for the fish gill pattern PHE, these values are obtained as 1881W, 20.26W/K and 0.18, respectively. It has been observed that the trachea pattern PHE is better in increasing the amount of heat transfer compared to the fish gill pattern PHE.

1 INTRODUCTION

A heat exchanger (HE) is one of the most essential equipment in thermal engineering applications. Due to its function and structure, it has a key importance in energy efficiency and sustainability (Dal, 2019). The essential improvements made for more efficient use of energy and efficiency in HEs are increasing heat transfer per unit volume and reducing the average temperature difference between fluids. Among the current literature, Gürel *et al.* (2020) designed a lung pattern on the plate surface based on the human lung with a biomimetic approach. Computational fluid dynamics (CFD) analysis was performed for 3kW compact plate heat exchanger (PHE) and classical chevron type PHE under the same boundary conditions and various correlations were derived. Sheikholeslami *et al.* (2015) experimentally investigated heat transfer and pressure drop in double pipe HEs using air and water. They placed typical circular ring and bore circular ring turbulators inside the annular tube and investigated the air flow for various Reynolds number (6,000-12,000), pitch ratio of holes (1.83, 2.92, and 5.83), and number of pitches (0-8). Accordingly, they derived correlations for friction factor, Nusselt number and thermal performance. Yıldırım *et al.* (2011) analyzed the thermal performance of the fluid in micro-channel HEs and examined its effect on temperature distribution and HE efficiency. Tsai *et al.* (2009) carried out a CFD analysis for the flow distribution and characteristics of the chevron type PHE in the cross-channels with a real-size 3D model and verified with experimental results. It was seen that the pressure drop calculated with CFD analysis is 20% less than the

experimental values. This is because of the irregular flow distribution at the duct inlets. Accordingly, it has been revealed that CFD studies to be carried out in such complex structures should be carried out with more mesh elements. One of the ways to improve the performance of PHEs is to increase the heat transfer surface area. In PHEs, this process is done by adding plates. However, the heat transfer area on each plate is also increased by using fins, grooves and guides. Therefore, in this study, the compact PHEs with two different surface geometries was handled. By using the biomimetic method, patterns were created on the plate surface, inspired by fish gill and trachea respiration. In this study, their verified CFD analysis have been carried out. The temperature and pressure distributions have been compared, and their convective heat transfer coefficient (h), Reynolds number (Re), Prandtl number (Pr), heat transfer amount (Q) and effectiveness (ε) have been discussed for both hot and cold sides. Crucial parameters that determine the amount of heat transfer and classify the flow characteristics in a HE are heat transfer between finite temperature levels, mixing of fluid and frictions. Phase change and flow throttling also affect the performance of HEs (Shah Ramesh *et al.*, 2003; Wark, 1995). All those parameters are great sources of irreversibility and directly determines the amount of entropy production which is the amount of entropy produced in any irreversible process such as the motion of bodies, heat exchange, fluid flow, expanding or mixing substances, heat and mass transfer processes, including anelastic deformation of solids (Karlsson, 1990). A typical Organic Rankine Cycle (ORC) should include at least two heat exchangers (a condenser and an evaporator). In ORC systems, overall efficiency is highly related with evaporator performance. Hence exchanger type and design are great concerns. PHEs are used in a broad range of engineering applications because of great heat transfer performance, compactness and relatively simple production process (Ayub, 2003). Furthermore, since it is easy to manipulate surface geometry in PHEs, it is possible to obtain a turbulent flow in lower Reynolds ranges comparing to other HE types. Many studies have been conducted in order to understand the heat transfer and pressure drop characteristics of the PHE as an evaporator. Since the working fluid undergoes a phase change in the evaporator, these studies mainly focused on the two-phase heat transfer and pressure drop properties of the PHE.

2 COMPACT PLATE HEAT EXCHANGER

Biomimicry is the adaptation of the movements and other functions of living organisms into the engineering applications. Various robots, machines, devices and systems are designed with this method (Biomimicry Guild, 2007). Trachea and fish gill patterns were engraved on the plate surface of a plate heat exchanger (PHE) using biomimetic in this study. The design of the PHE consisting of 125.5mm x 431mm 3-plate was analyzed by CFD simulation. The effect of plate pattern on heat transfer and pressure drop have been investigated. The plate surface geometry is designed as a 3D fish gill as shown in Figure 1.

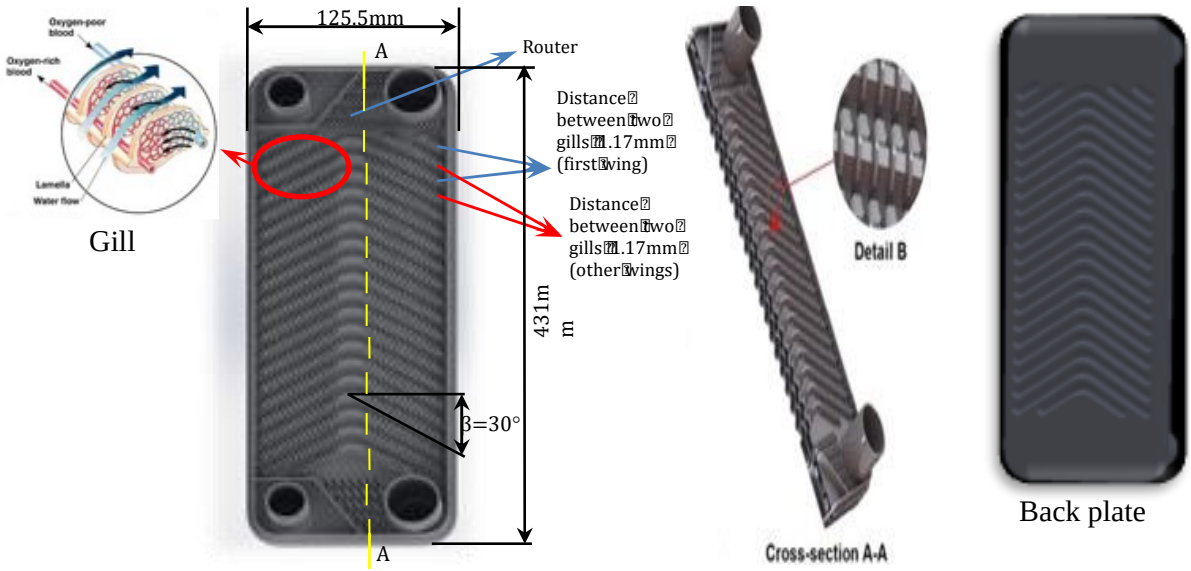

Figure 1. Geometric details of fish grill pattern compact PHE designed.

In Figure 1, plate surface angle is chosen as 30°. There are 21 chevron angled wings (0.35mm of width and 1.7mm of height) on the plate surface which mimic gills of a fish. On the very first wing distance between gills are 1.17mm. However, it is 1.43mm for the rest in order to prevent the flow being blocked. Routers (0.48mm in width and separated by 1.5mm) have been added at the wings-free locations on the plate surface. Designed PHE is consist of three plates of 4mm in thickness. Compactness which is defined as heat transfer surface area scaled by the heat exchanger volume (m^2/m^3) is an important design parameter for heat exchangers. Compactness value of the design used in this study have been calculated as 6280.

3D trachea shaped hemispherical fins with a diameter of 3.60mm and height of 1.60mm are designed for the plate surface. As seen in Figure 2, both sides of the plate surface are covered with a trachea pattern. 16 routers are added in the form of capsules on the hot inlet and outlet sleeves. The diverters are provided to distribute the incoming and outgoing flow homogeneously. With this geometry, the compactness value of the PHE reached to 8150.

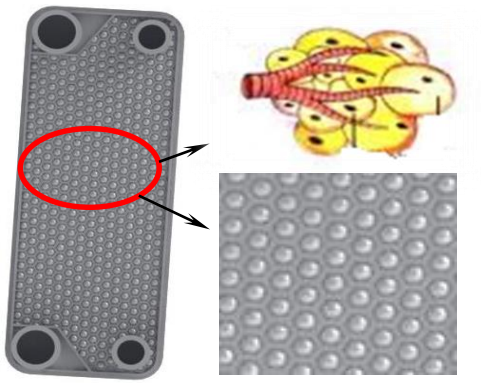

Figure 2. Design of trachea pattern compact PHE.

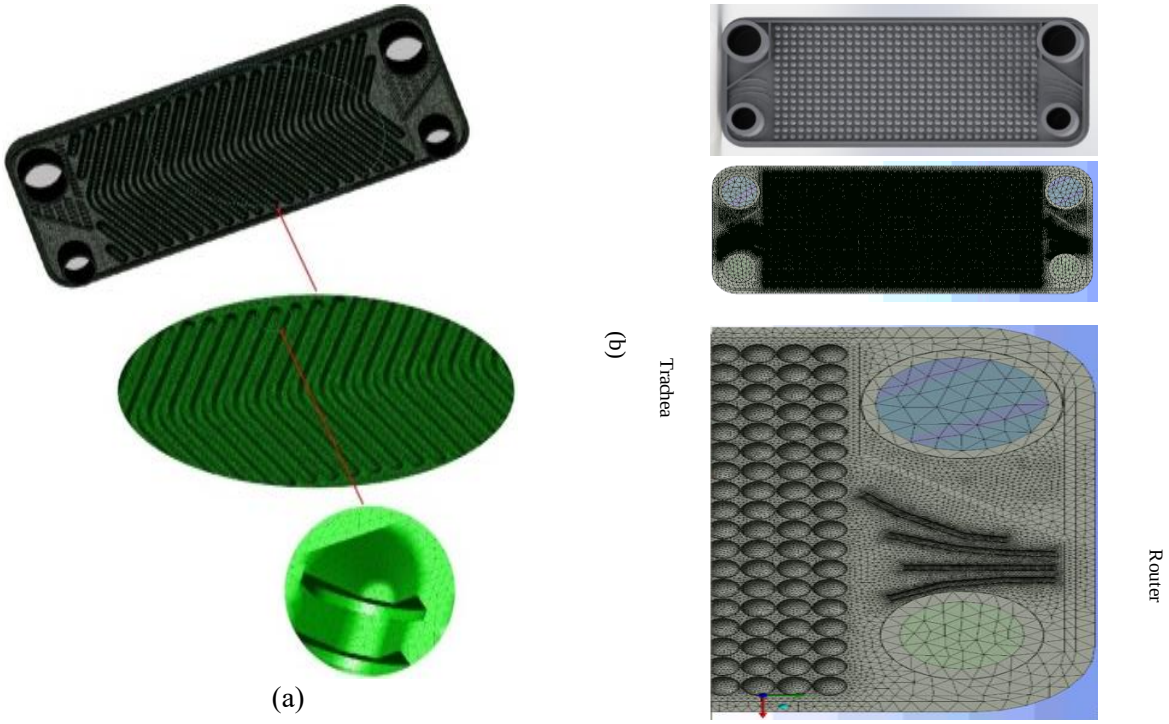

Figure 3. Mesh structures of (a) fish gill design and (b) trachea design.

Mesh structures of the designs were constructed using ANSYS-Meshing (Ansys Fluent, 2017) (Figure 3). SIMPLE algorithm was used in numerical analysis and standard k-epsilon, turbulence equation was used with reference to literature studies (Gürel *et al.*, 2020). 10 million tetrahedral elements were

used for the fish gill pattern. This is 11 million for the trachea pattern.

3 ANALYSIS

PHE is a device that allows the passage of the hot fluid on one side and the cold fluid on the other side and provides the heat exchange between these two fluids. In this study, two different HEs were designed by designing grooves in the form of a trachea pattern and a fish gill on the plate surface. These PHEs consist of 3 plates each. Dimensions and boundary conditions of designed PHEs are given in Table 1. In addition, water was used as the working fluid in this study. These boundary conditions were applied to Ansys-Fluent 18 which is based on the finite volume method and the following equations (Ansys Fluent, 2017). Simulation parameters are given in Table 2.

Table 1. Design parameters of compact PHEs

	Chevron type (30°)	**Trachea pattern**	**Fish gill pattern**
The length of the compact HE, H (mm)	431	192	192
The width of the compact HE, W (mm)	125.5	74	74
Number of plates	10	3	
Hot water inlet temperature, $T_{h,in}$ (°C)	32.8	90	
Cold water inlet temperature, $T_{c,in}$ (°C)	25	40	
Environment temperature, T_0 (°C)	-	27	
Mass flow rate, $\dot{m}$ (kg/s)	0.167	0.05	

Continuity equation:

$$\frac{\partial(\rho u)}{\partial x}+\frac{\partial(\rho v)}{\partial y}+\frac{\partial(\rho w)}{\partial z}=0 \tag{1}$$

Momentum equation:

$$u\frac{\partial(\rho u)}{\partial x}+v\frac{\partial(\rho v)}{\partial y}+w\frac{\partial(\rho w)}{\partial z}=-\frac{\partial P}{\partial x}+\mu\left[\frac{\partial^2 u}{\partial x^2}+\frac{\partial^2 u}{\partial y^2}+\frac{\partial^2 u}{\partial z^2}\right] \tag{2}$$

$$u\frac{\partial(\rho u)}{\partial x}+v\frac{\partial(\rho v)}{\partial y}+w\frac{\partial(\rho w)}{\partial z}=-\frac{\partial P}{\partial y}+\mu\left[\frac{\partial^2 v}{\partial x^2}+\frac{\partial^2 v}{\partial y^2}+\frac{\partial^2 v}{\partial z^2}\right] \tag{3}$$

$$u\frac{\partial(\rho u)}{\partial x}+v\frac{\partial(\rho v)}{\partial y}+w\frac{\partial(\rho w)}{\partial z}=-\frac{\partial P}{\partial z}+\mu\left[\frac{\partial^2 w}{\partial x^2}+\frac{\partial^2 w}{\partial y^2}+\frac{\partial^2 w}{\partial z^2}\right] \tag{4}$$

Energy equation:

$$u\frac{\partial(\rho T)}{\partial x}+v\frac{\partial(\rho T)}{\partial y}+w\frac{\partial(\rho T)}{\partial z}=-\frac{\partial P}{\partial x}+\mu\left[\frac{\partial^2 T}{\partial x^2}+\frac{\partial^2 T}{\partial y^2}+\frac{\partial^2 T}{\partial z^2}\right] \tag{5}$$

Table 2. Simulation parameters

simulation condition	**steady-state**
solver type	pressure based
mesh structure/mesh number	tetrahedral/10 millions
turbulence model	standard k-ε turbulence model
wall–turbulence interaction	standard wall-function
pressure–velocity coupling	SIMPLE algorithm
discretization method	second order upwind

Wall functions are based on *Law of the Wall* in which turbulence near the boundary is a function only of the flow conditions pertaining at the wall and is independent of the flow conditions further away. In the evaluation of the applicability of wall functions, one of the most important parameters is dimensionless wall distance (y^+) (Schlichting and Gersten, 2016). In order to evaluate estimated wall distance (Δs), fluid velocity, density (ρ) and dynamic viscosity (μ) must be known.

The accuracy of the simulation results depends on the mesh quality. Accordingly, the appropriate mesh size was calculated with the y^+ calculations detailed below. The average Reynolds (Re) number between plates was calculated as 1470. Then the flow is transitional. For a more precise calculation, y^+ value was taken as 5 in this study. According to the design parameters and fluid properties given in Table 3, Δs is calculated as 0.00015m.

$$\mathrm{Re_x} = \frac{\rho U_\infty L}{\mu} \tag{6}$$

$$C_f = \frac{0.026}{\mathrm{Re_x^{1/7}}} \tag{7}$$

$$T_{wall} = \frac{C_f \rho U_\infty^2}{2} \tag{8}$$

$$U_{fric} = \sqrt{\frac{T_{wall}}{\rho}} \tag{9}$$

$$\Delta s = \frac{y^+ \mu}{U_{fric} \rho} \tag{10}$$

Table 3. The design parameters and fluid properties in compact PHEs.

Parameters	Values	Parameters	Values
U_∞ (m/s)	0.49	L (m)	0.003
ρ (kg/m^3)	1000	y+	5
μ (kg/m-s)	0.001	Δs (m)	0.00015
Re_x		1470	

Heat rate in a HE is give as:

$$q = \varepsilon(\dot{m}c_p)_{min}(T_{h,in} - T_{c,in}) \tag{11}$$

where effectiveness is $\varepsilon = q/q_{max}$.

3.1 Verification

Kilic (2013) performed the thermodynamic analysis of a gasketed PHE consisting of angled chevron at 30° both numerically and experimentally. The design parameters of the PHE used in that study are shown in Table 1. Mesh of the numerical model consists of 24 million tetrahedral elements. Trachea pattern and fish gill pattern designs examined in this study were verified by Kilic (2013)'s study.

Temperature and pressure distributions of hot side in the reference study are given in Figure 4. According to the numerical result with k-ε turbulence model, hot inlet and outlet temperatures are 32.8°C and 29.6°C respectively and temperature difference is 3.1°C. Outlet temperature in experimental study is 29.9°C. Hence deviation between numerical and experimental results is 7.7%. Inlet and outlet gauge pressures are 5800Pa and 1050Pa respectively. Outlet pressure is measured 1120Pa (gauge) in the experimental study. Hence deviation between simulation and experimental results is 1.47%. The comparison of the numerical and experimental results of the reference study is given in Table 5. The amount of heat transfer is 2143W and 2167W, for numerical and experimental studies respectively. The results are consistent since the deviation is only 1.11% Thus, the suggested k-ε turbulence model is valid in such systems and can be used in this study too.

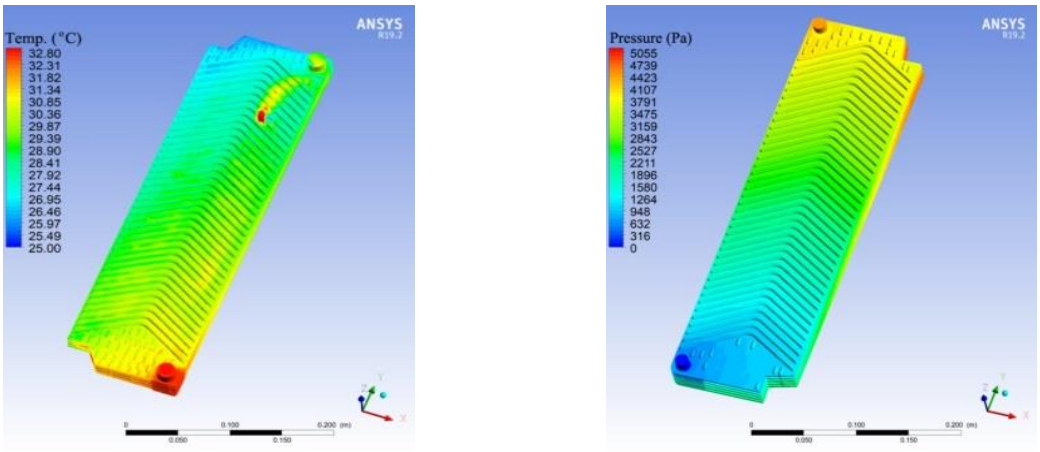

(a) (b)

Figure 4. Temperature distribution in the reference PHE in (a) hot side and (b) cold side

Table 4. Comparison of experimental and simulation results

Parameters	Value
Heat transfer rate (experimental) (W)	2167
Heat transfer rate (simulation) (W)	2143
Error, (%)	1.11

4 RESULTS AND DISCUSSION

Temperature distributions at the hot side surface in trachea design is shown in Figure 5(a). Fluid inlet temperature is 90°C and drops to at 88–89°C, at inlet router. A dead zone is observed in the upper right corner of the plate where the temperature drops to 71°C. The temperature in the middle parts of the trachea pattern is around 81°C. This temperature drop continues until the end of the plate where the temperature is approximately 78°C. Dead zones are also observed in the lower right corner of the plate and the temperature in this zone is approximately 70°C. Occurrence of dead zones indicates flow velocity at those zones are low. In order to increase heat transfer router arrangements should be optimized. The outlet temperature is calculated as 76.6°C. The temperature difference between inlet and outlet is 13.4°C.

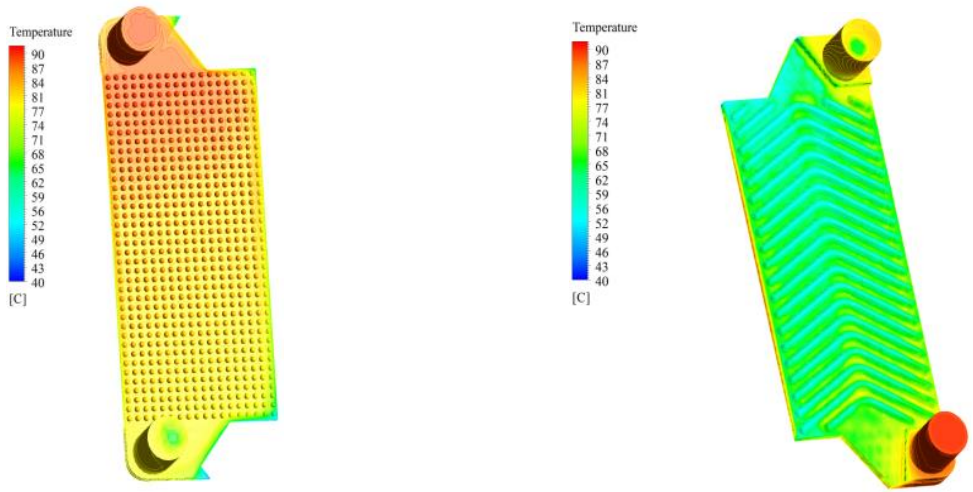

(a) (b)

Figure 5. Temperature counters at hot side for (a) trachea design and (b) fish gill design.

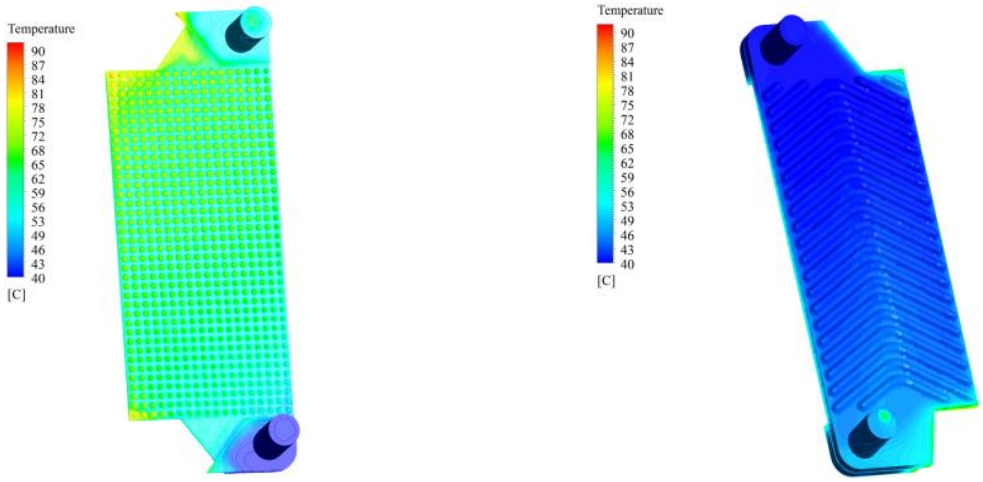

(a) (b)

Figure 6. Temperature counters at cold side for (a) trachea design and (b) fish gill design.

The temperature distribution obtained in fish gill design is given in Figure 5(b). Inlet temperature is 90°C. The fluid flows into the fish gill pattern, dropping its temperature to 86°C in the routers. For

edge zones, from the entrance of the pattern to the middle part, the temperature drops to 70°C. It changes between 68-62°C from the middle part to the pattern exit. In routers, the temperature dropped to about 82°C. The flow leaves the plate by decreasing its temperature up to 81°C at the outlet. Total temperature drop is 9°C. Similar behaviors have been observed in the side of the exchangers as given in Figure 6. According to these results, the trach design provides more temperature reduction, but the dead zones formed need to be improved.

The pressure (gauge) distributions obtained for the hot and cold sides in the designed heat exchangers are shown in Figures 7 and 8. Similar pressure gradient was observed on the hot and cold sides for both designs. In the hot side, pressure drop in trachea design is approximately 8000Pa (9000Pa inlet, 1000Pa outlet). In fish gill design, this value is much lower (2500Pa). Exactly same behavior is observed for the cold side. Hence according to these results, it was revealed that the trachea design provides better heat transfer, but it should be heavily improved in terms of pressure drop.

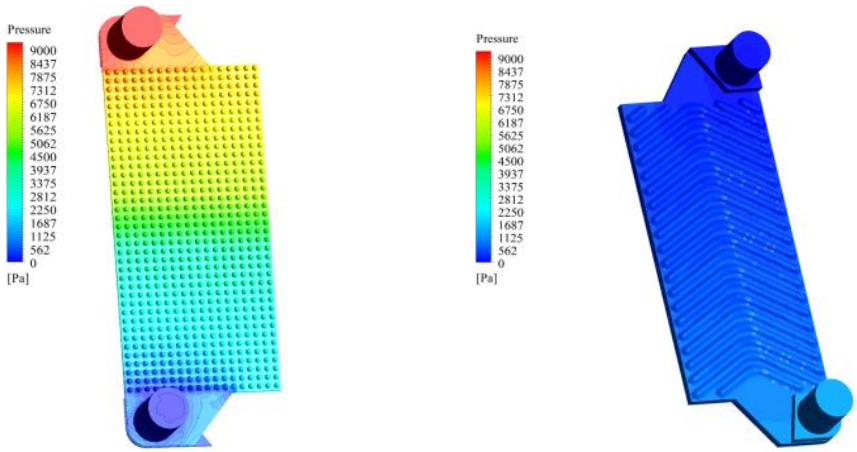

(a) (b)

Figure 7. Pressure distributions at hot side for (a) trachea design and (b) fish gill design.

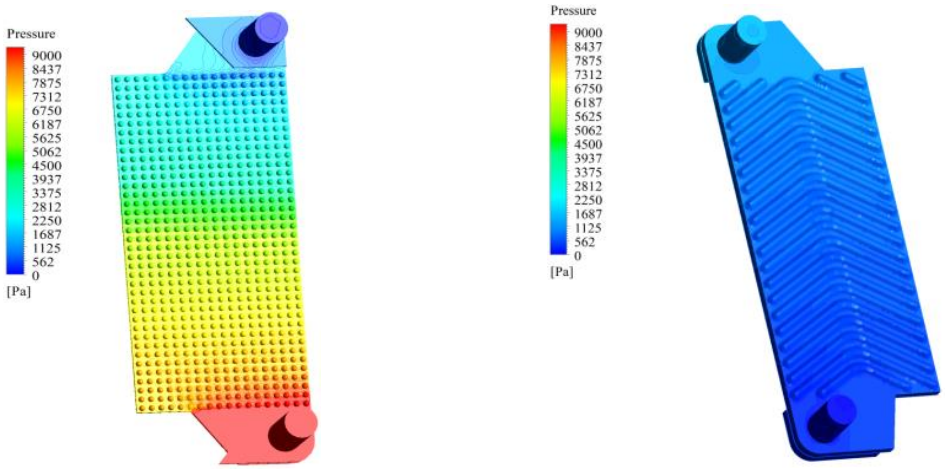

(a) (b)

Figure 8. Pressure distributions at cold side for (a) trachea design and (b) fish gill design.

In Table 5, the convective heat transfer coefficients (h), Reynold (Re) and Prandtl (Pr) numbers calculated for both hot and cold sides are given. The purpose of the plate surface designs focused in this study is to create a turbulent flow and increase the amount of heat transfer. As expected, the heat transfer that took place in the more turbulent flow was higher. It was observed that the h and Pr values of the fish gill design is higher. Pr values for the hot and cold sides is calculated as 2.08 and 3.95, respectively. These values are 2.03 for the hot side and 3.78 for the cold side in trachea design. In both designs, it was observed that h and therefore Pr were higher on the cold side.

Table 5. Calculated heat transfer co-efficient (h), Reynolds (Re) and Prandtl (Pr) numbers.

Parameters	Trachea		Fish Gill	
	Hot side	Cold side	Hot side	Cold side
h (W/m^2 K)	21785.4	18038	7691.42	6283.17
Re	43486.5	24476	24027.01	13225.44
Pr	2.03	3.78	2.06	3.95

Amount of heat transfer, effectiveness, compactness, entropy generation, hydraulics diameters calculated in both heat exchanger designs are shown in Table 6. It is seen that the trachea design is better in terms of heat transfer amount and efficiency value because of greater temperature difference between inlet and outlet. ΔT is 13.5°C in trachea design and 9°C in fish gill design. In addition, the effectiveness of a heat exchanger depends on the geometry of the heat exchanger as well as on the flow regime. Therefore, trachea design in which effectiveness is higher has also the highest compactness. Generated entropy is 27.07W/K and 20.26W/K in trachea and fish gill design, respectively. This is mainly due to compactness. Since trachea design is more compact, irreversibility due to friction is high.

Table 6. Heat transfer amount, efficiency and entropy generation values of compact PHEs.

Parameters	Trachea pattern	Fish gill pattern
Heat transfer, Q (W)	2800	1881
Effectiveness, ε	0.267	0.18
Compactness	8150	6280
Entropy generation, S_{gen} (W/K)	27.07	20.26
Hot side hydraulic diameter (mm)	0.018	0.018
Cold side hydraulic diameter (mm)	0.013	0.013
Total heat transfer surface (mm^2)	1696	942
Hot side average velocity (m/s)	0.308	0.973
Cold side average velocity (m/s)	0.314	0.995

5 CONCLUSION

In this study, two different plate patterns (trachea and fish gill) were designed and analyzed for a plate heat exchanger consisting of 3-plates. CFD simulations were conducted for specific inlet temperatures (90°C for hot inlet and 40°C for cold inlet) and 0.05kg/s flowrate. Water was used as the working fluid. The following results were obtained. A higher compactness value has been achieved with the trachea design.

- As a result, the heat transfer realized in the tracheal design was 48% higher than in the fish gill design.
- Consequently, the heat transfer realized was 48% higher than in the fish gill design.
- The resulting temperature change is 50% greater in trachea design.
- On the other hand, pressure drop in the tracheal design was higher than in the other design.
- Entropy production is 33% higher in trachea design.

As a result of the study, hot spots of both designs were revealed. The next work will be on optimizing the designs in line with the findings.

REFERENCES

Ansys Fluent 18.0, User's Guide, ANSYS Inc., 2017.

Biomimicry Guild, Innovation Inspired by Nature Work Book, April, 2007.

Dal, A.R., 2019, Numerical analysis of optimum blade range of a flat-plate tube heat exchanger. *Nigde Omer Halisdemir Uni. J. Eng. Sci.*, 8(1), 479-501.

Genceli, O., 1999, Isı Değiştiricileri. Birsen Yayınevi, İstanbul, Turkey, [in Turkish].

Gürel, B., Akkaya, V.R., Göltaş, M., Şen, Ç.N., Güler, O.V., Koşar, M.İ., Keçebaş, A. 2020, Investigation on flow and heat transfer of compact brazed plate heat exchanger with lung

pattern. *Appl. Therm. Eng.*, 115309.
Karlsson, S. (1990). Energy, entropy and exergy in the atmosphere. Chalmers University of Technology.
Kilic, B. (2013). Experimental investigation of effects to heat transfer of plate geometry with dynamic and thermal parameters in the plate heat exchangers (Doctoral dissertation, Ph. D. thesis. Süleyman Demirel University, The Graduate School of Natural and Applied Sciences, Isparta, Turkey.
Kilic, B., Ipek, O., 2017, Experimental investigation of heat transfer and effectiveness in corrugated plate heat exchangers having different chevron angles. *Heat Mass Trans.*, 53(2), 725-731.
Li, J., Yang, Z., Hu, S., Yang, F., & Duan, Y. (2020). Effects of shell-and-tube heat exchanger arranged forms on the thermo-economic performance of organic Rankine cycle systems using hydrocarbons. *Energy Conv. Manage.t*, 203, 112248.
Luo, X., Huang, R., Yang, Z., Chen, J., & Chen, Y. (2018). Performance investigation of a novel zeotropic organic Rankine cycle coupling liquid separation condensation and multi-pressure evaporation. *Energy Conv. Manage.*, 161, 112-127.
Shah Ramesh, K., Sekulic Dušan, P. 2003. Fundamentals of Heat Exchanger Design, p.755, John Wiley & Sons Inc., USA.
Sheikholeslami, M., Gorji-Bandpy, M., Ganji, D.D., 2015, Experimental study on turbulent flow and heat transfer in an air to water heat exchanger using perforated circular ring. *Exper. Therm. Fluid Sci.*, 70, 185-195.
Schlichting, H., & Gersten, K. (2016). Boundary-layer theory. Springer.
Tsai, Y.C., Liu, F.B., Shen, P.T., 2009, Investigations of the pressure drop and flow distribution in a chevron-type plate heat exchanger. *Int. Commun. Heat Mass Trans.*, 36 (6), 574-578.
Yildirim, O., Guo, Z., 2011, High-efficiency micro channel regenerative heat exchanger for fluid processing, in: Comsol User Conference.
Wark, K. 1995. Advanced Thermodynamics for Engineers, pp. 85-120, McGraw-Hill Inc., USA.

ACKNOWLEDGEMENT

The authors gratefully acknowledge the support provided by the Turkey Scientific and Technological Research Council (TUBITAK) under the project number 218M470.